CMLS Cellular and Molecular Life Sciences

Research Article

Increased apoptosis in differentiating p27-deficient mouse embryonic stem cells

V. Bryja[a,b] **J. Pacherník**[a,c]**, K. Souček**[d]**, V. Horvath**[d]**, P. Dvořák**[a–c] **and A. Hampl**[a–c,]*

[a] Center for Cell Therapy and Tissue Repair, Charles University, V Uvalu 84, 150 06 Prague (Czech Republic)
[b] Department of Molecular Embryology, Institute of Experimental Medicine, Academy of Sciences of the Czech Republic, Videnska 1083, 142 20 Prague (Czech Republic)
[c] Laboratory of Molecular Embryology, Mendel University Brno, Zemedelska 1, 613 00 Brno (Czech Republic), Fax + 420 545 133 298, e-mail: hampl@mendelu.cz
[d] Institute of Biophysics, Academy of Sciences of the Czech Republic, Kralovopolska 135, 656 53 Brno (Czech Republic)

Abstract. In mouse embryonic stem (mES) cells, the expression of p27 is elevated when differentiation is induced. Using mES cells lacking p27 we tested the importance of p27 for the regulation of three critical cellular processes: proliferation, differentiation, and apoptosis. Although cell cycle distribution, DNA synthesis, and the activity of key G1/S-regulating cyclin-dependent kinases remained unaltered in p27-deficient ES cells during retinoic acid-induced differentiation, the amounts of cyclin D2 and D3 in such cells were much lower compared with normal mES cells. The onset of differentiation induces apoptosis in p27-deficient cells, the extent of which can be reduced by artificially increasing the level of cyclin D3. We suggest that the role of p27 in at least some differentiation pathways of mES cells is to prevent apoptosis, and that it is not involved in slowing cell cycle progression. We also propose that the pro-survival function of p27 is realized via regulation of metabolism of D-type cyclin(s).

Mouse embryonic stem (mES) cells are a unique cell type derived from the inner cell mass of pre-implantation blastocysts [1, 2]. The defining feature of mES cells is their ability to follow multiple differentiation pathways both in vivo and in vitro [3]. Such differentiation is underlined by the coordinated induction and repression of many genes [4] with concomitant changes in cell phenotype. The most prominent effect of differentiation is reduced proliferation and altered cellular morphology.

The cyclin-dependent kinase (CDK) inhibitor p27[Kip1] (here referred to as p27) is one of the proteins induced when mES cells enter a differentiation pathway [5]. This up-regulation of p27 occurs in all differentiating mES [and also in closely related embryonal carcinoma (EC) cells], regardless of cell line or differentiation conditions [5–12]. Because p27 up-regulation invariably occurs, it is likely to be of specific importance for the differentiation of cells of early embryonic origin. In such cell types, p27 is responsible not only for halting proliferation [5, 6, 8, 13] but also for affecting other aspects of differentiation [6, 11, 13], as well as apoptosis [8, 13]. However, with one exception [5], all p27 functional studies have been performed in mouse EC cells rather than mES cells. Since EC cells differ from mES cells in some aspects of their biology, the relevance of such data for mES cells may be limited.

---

* Corresponding author.

In this study, newly established p27-deficient mES cell lines were used to explore the role of p27 in three distinct components of the differentiation process: i) changes in proliferation; ii) expression of differentiation markers, and iii) occurrence of apoptosis. In vitro differentiation into extraembryonic endoderm was induced by withdrawal of leukemia inhibitory factor (LIF) combined with treatment with retinoic acid (RA) in the presence of serum [14] to analyze these specific processes in both normal and p27-deficient mES cells. The data demonstrate that p27 is not required for either the arrest of proliferation or the expression of differentiation markers. However, as p27-deficient mES cells undergo massive apoptosis, we infer that p27 is crucial for some responses to differentiation-inducing conditions, such as cell survival following differentiation-inducing conditions.

Material and methods

Cell lines

Blastocysts resulting from crossing males and females of the same p27+/– genotype [15] were used for establishing p27-deficient mES cells using a standard protocol [16]. A polymerase chain reaction designed by Fero and colleagues [15] was used to determine the genotype of the established mES lines. Mouse ES cell line D3 derived by Doetschman et al. [17] was used for comparison.

Cell culture

Undifferentiated mES cells were propagated in Dulbecco's modified Eagle medium supplemented with 20% fetal calf serum, 100 mM nucleosides, 0.05 mM β-mercaptoethanol, 100 I.U./ml penicillin, 0.1 mg/ml streptomycin, and 1000 U/ml LIF, on gelatinized tissue culture dishes with or without mitomycin C-treated mouse embryonic fibroblasts (MEFs) as feeder layers.

Growth curves

Cells were seeded at a density of 5000 cells/cm^2 on MEFs and analyzed daily. Dishes with only MEFs were used as a blank for each day of the experiment.

Differentiation protocol

Cells were induced to differentiate as described by Savatier and colleagues [5]. Briefly, cells were seeded at a density of 10,000 cells/cm^2, LIF was withdrawn, and after 1 day they were treated with 10^{-6} M RA for 2 days. Culture medium was exchanged at day 1 and day 3. RA was prepared as a 5 mM stock solution in ethanol, then diluted in culture medium to a final concentration of 10^{-6} M.

Treatment with caspase inhibitors

The following inhibitors of caspases were used: Z-Val-Ala-DL-Asp(OMe)-fluoromethylketone   (Z-VAD-fmk,

general caspase inhibitor; Bachem, Bubendorf, Switzerland), Z-Asp(OMe)-Glu(OMe)-Val-DL-Asp(OMe)-fluoromethylketone (Z-DEVD-fmk, caspase 3 inhibitor; Bachem, and Z-Val-Glu(OMe)-Ile-Asp(OMe)-fluoromethylketone (Z-VEID-fmk, caspase 6 inhibitor; Sigma, St. Louis, Mo.). The inhibitors were added at day 1 of differentiation (described above) at a final concentration of 25 µM. For Western blot analysis, cells were harvested at day 3 of differentiation (following 48 h treatment).

Growth rate

The increase in total cellular protein was used as a measure of cell growth. Cells on culture dishes were washed twice with phosphate-buffered saline (PBS, pH 7.4) and lysed in 100 mM Tris/HCl (pH 6.8), 20% glycerol, and 1% SDS. Protein concentrations determined by a DC Protein Assay kit (Bio-Rad, Hercules, Calif.) were used to calculate the total amount of protein per dish.

Analysis of cell cycle distribution and DNA synthesis

Cells were harvested by trypsinization and fixed in 70% ethanol. DNA was stained by incubation (37°C, 30 min) with Vindelov's solution (10 mM Tris buffer, pH 8, 0.7 mg/ml RNase, 50 µg/ml propidium iodide, 0.1% Triton-X 100; 10 mM NaCl) [18]. For the analysis of DNA synthesis, the cells were labeled with 10 µM 5-bromo-2′-deoxy-uridine (BrdU) for 60 min under standard culture conditions (37°C, 5% CO_2, 95% humidity). After labeling, the cells were trypsinized and fixed in 70% ethanol at 4°C overnight. Following fixation, the cells were washed with PBS and incubated in 2 M HCl with 0.5% Triton X-100 at 37°C for 1 h. The cells were pelleted by centrifugation at 500 g for 10 min, resuspended in 0.1 M sodium borate (pH 8.5), and incubated at room temperature (RT) for 10 min. After another round of centrifugation, the cells were resuspended in PBS supplemented with 1% bovine serum albumin (BSA), 0.5% Triton X-100 to 10^6 cells/100 µl. The anti-BrdU antibody conjugated with fluorescein isothiocyanate (FITC; BD Pharmingen 556028, San Diego, Calif.) was added to the cell suspension at a 1:10 ratio and incubated overnight at 4°C. The samples were washed in PBS with 1% BSA and DNA was labeled with propidium iodide (50 µg/ml propidium iodide, 0.7 mg/ml RNase). DNA content and synthesis were analyzed using flow cytometry (argon ion laser, 488 nm for excitation, FACSCalibur; Becton Dickinson, San Jose, Calif.). For each sample, 1.5×10^4 cells were acquired. The percentages of cells in the individual cell cycle phases were analyzed using ModFit 2.0 software (Verity Software House, Topsham, Me.). CellQuest 3.1 (Becton Dickinson) software was used for DNA synthesis analysis. Single cells were identified and gated by pulse-code processing of the area and width of the signal. Cell debris was excluded by appropriately raising the forward scatter threshold.

Alkaline phosphatase staining

Colonies of mES cells grown on MEFs were washed with PBS and fixed with 4% paraformaldehyde in PBS (pH 7.4) for 15 min. After washing with distilled water (5 min), the cells were incubated in 0.45-µm-filtered 100 mM Tris/HCl (pH 8.5) with naphthol-AS-BI phosphate (250 µg/ml) and Fast Red Violet LB (250 µg/ml). The reaction was stopped by washing with distilled water, and samples were analyzed immediately.

Western blotting

For Western blot analysis, cell samples were prepared as follows. Cells on a culture dish were washed twice with PBS (pH 7.4) and lysed in 100 mM Tris/HCl (pH 6.8), 20% glycerol, and 1% SDS. Protein concentrations were determined by a DC Protein Assay kit (Bio-Rad, Hercules, Calif.). Equal amounts of total protein were subjected to 10% SDS PAGE, electrotransferred onto Hybond-P membrane, immunodetected using appropriate primary and secondary antibodies, and visualized by ECL+Plus reagent according to the manufacturer's instructions (Amersham, Aylesbury, UK). When required, membranes were stripped in 62.5 mM Tris/HCl (pH 6.8), 2% SDS, and 100 mM β-mercaptoethanol, washed, and reblotted with another antibody. When required, the intensities of signals were assessed by densitometry using Intelligent Quantifier software (BioImage, Ann Arbor, Mich.). After immunodetection, each membrane was stained with amidoblack to confirm equal protein loading. The antibodies used were as follows. Mouse monoclonal antibody to cyclin D1 (sc-450), rabbit polyclonal antibodies to Bcl-2 (sc-492), Bcl-X$_L$ (sc-7195), Oct-4 (sc-9081), PARP (sc-7150), and p21 (sc-397), and goat polyclonal antibody to lamin B (sc-6217) were purchased from Santa Cruz Biotechnology (Santa Cruz, Calif.); mouse monoclonal antibodies to p27 (K25020) and Bad (B31420) were purchased from Transduction Laboratories (Lexington, Ky.); mouse monoclonal antibodies to cyclin A (Ab-1, E23), cyclin D2 (Ab-4, DCS-3.1 + DCS-5.2), and Bag-1 (Ab-1, 3.9F1E11) were purchased from Neomarkers (Fremont, Calif.); rabbit polyclonal antibody to Bak (556396) was purchased from Pharmingen (San Diego, Calif.); mouse monoclonal antibody to alpha tubulin (Tu-01) was provided by Dr P. Draber (Institute of Molecular Genetics, Prague, Czech Republic); mouse monoclonal antibody to a C-terminal part of cyclin D3 (DCS-22) was provided by Dr J. Lukas (Danish Cancer Society, Copenhagen, Denmark), and mouse monoclonal antibody to p21 (Waf1) was provided by Dr B. Vojtesek (Masaryk Memorial Cancer Institute, Brno, Czech Republic). The hybridoma TROMA-I developed by Drs P. Brulet and R. Kemler was obtained from the Developmental Studies Hybridoma Bank developed under the auspices of the NICHD and maintained by The University of Iowa, Department of Biological Sciences, Iowa City, Iowa.

Immunoprecipitation and kinase assays

For these assays, cells were extracted for 30 min in ice-cold lysis buffer [50 mM Tris/HCl, pH 7.4, 150 mM sodium chloride, 0.5% Nonidet P-40, 1 mM ethylenediaminetetraacetic acid (EDTA), 0.1 mM dithiothreitol, 50 mM sodium fluoride, 8 mM β-glycerophosphate, 100 mM PMSF, 1 µg/ml leupeptin, 1 µg/ml aprotinin, 10 µg/ml soybean trypsin inhibitor, 10 µg/ml tosylphenylalanine chloromethane]. Extracts were cleared by centrifugation at 15,000 g for 15 min at 4 °C and stored at −80 °C until use. Concentrations of total protein were determined using a DC Protein Assay Kit (Bio-Rad). The extracts were first subjected to initial absorption with Protein G agarose beads and then incubated with appropriate antibodies for 1 h in an ice bath. Rabbit polyclonal antibodies to cyclin A (sc-751), cyclin E (sc-481), CDK4 (sc-260), and p27 (sc-528) and goat polyclonal antibodies to CDK 2 (sc-163-G), and CDK 4 (sc-601-G, for kinase assay only) were purchased from Santa Cruz Biotechnology and used in immunoprecipitation studies. Immunoprecipitates were collected on Protein G agarose beads by overnight rotation, washed four times with lysis buffer, resuspended in 2× Laemmli sample buffer and subjected to SDS-PAGE followed by Western blot analysis. For kinase assays, immunoprecipitates were prepared as above, except that the last two washes were done using kinase assay buffer (50 mM HEPES, pH 7.5, 10 mM MgCl$_2$, 10 mM MnCl$_2$, 8 mM β-glycerophosphate; 1 mM dithiothreitol). For CDK2, kinase reactions were carried out for 30 min at 37 °C in a total volume of 25 µl in kinase assay buffer supplemented with 100 µg/ml histone H1 (type III-S) and 40 µCi/ml [^{32}P]ATP. For CDK4, kinase reactions were carried out for 30 min at 30 °C in a total volume of 25 µl in kinase assay buffer supplemented with 160 µg/ml GST-pRb (type III-S) and 40 µCi/ml [^{32}P]ATP. Reactions were terminated by addition of 2× Laemmli sample buffer, and each reaction mix was subjected to SDS-PAGE and autoradiography. When required, signal intensities were assessed by densitometry using Intelligent Quantifier software (BioImage, Jackson, Mich.).

Indirect immunofluorescence

For indirect immunofluorescence (IIF), cells were grown on glass cover slips and fixed in 95% ethanol/1% acetic acid for 30 min on ice, then slowly rehydrated, quenched with 1% BSA in PBS for 1 h at RT, incubated with the appropriate primary (overnight at 4 °C) and FITC-conjugated secondary (1 h, RT) antibodies and mounted to Mowiol (Hoechst, Frankfurt, Germany). The antibodies used were as follows: rat monoclonal antibody to cytokeratin Endo-A (TROMA-I; see Western blotting), mouse monoclonal antibody to SSEA-1 (Tec-1) provided by Dr P. Draber (Institute of Molecular Genetics, Prague, Czech Republic), and mouse monoclonal antibody to E-cad-

herin (C20820; Transduction Laboratories). Microscopice analysis was performed using an upright Olympus BX60 microscope equipped with a Fluoview confocal laser scanning system.

DNA fragmentation analysis

One million cells were washed in PBS (pH 7.4), resuspended in 400 µl lysis buffer (100 mM NaCl, 25 mM EDTA, pH 8.0, 10 mM Tris/HCl, 0.5% SDS) and incubated overnight with proteinase K (0.5 µg/µl). The next day, RNase (100 µg/µl) was added for 2 h at 37°C, and the sample was precipitated with 400 µl of 5 M NaCl and subsequently cleared by centrifugation. DNA in supernatant was precipitated with 560 µl isopropanol, diluted in TE buffer (10 mM Tris/HCl, pH 8.0, 1 mM EDTA) and analyzed on a 1.5% agarose gel.

TUNEL assay

Cells were trypsinized, washed with PBS (pH 7.4), and collected by centrifugation. The cell pellet was resuspended in culture medium (0.5 ml), added dropwise to cold 1% paraformaldehyde (5 ml), and incubated for 15 min on ice. After another wash with PBS (pH 7.4), the cells were transferred to 70% ethanol and stored at −20°C until use. For the TUNEL assay, fixed cells were washed with PBS+0.1% BSA (pH 7.4), resuspended in 50 µL of TUNEL reaction mixture (In Situ Cell Death Detection Kit, Fluorescein, Roche, Basel, Switzerland), and incubated overnight in the dark. After washing once with 1.5 ml rinsing buffer (0.1% v/v Triton X-100 + 5 mg/ml BSA in PBS, pH 7.4), the cells were resuspended in 1 ml of freshly prepared propidium iodide (PI) staining solution (5 µg/ml PI + 200 µg/ml RNase in PBS, pH 7.4) and incubated for 30 min at RT in the dark. The samples were analyzed using flow cytometry as described in Analysis of cell cycle distribution and DNA synthesis.

Transient transfection and analysis of mitochondrial membrane potential

Cells were electroporated as described previously [19] with a mixture (1:8) of pEGFP-C1 (BD Biosciences Clontech, Palo Alto, Calif.) and pNeoCycD3 [10] expression vectors. The effect of the transfection on apoptosis was evaluated by measuring changes in mitochondrial membrane potential ($\Delta\Psi_m$). Briefly, cells were washed twice with Hank's balanced salt solution without calcium and magnesium ions (HBSS), resuspended in 100 mM tetramethylrhodamine ethyl ester perchlorate (TMRE; Molecular Probes, Eugene, Or.) in HBSS (approximately 10^6 cells/ml), and incubated for 20 min at RT in the dark. At the end of the incubation period, cells were washed in HBSS, resuspended in a total volume of 500 ml HBSS, and at least 10^5 cells were analyzed using a FACSCalibur flow cytometer and CellQuest 3.1 software (Becton Dickinson). Data are expressed as the percentage of cells with

a negative TMRE fluorescence from a GFP-positive population.

Results

Characterization and growth properties of p27-deficient mES cells

Wild-type and p27-deficient blastocysts were obtained by crossing mice that were heterozygous for p27 [15]. As determined by PCR, two independent p27+/+ and three independent p27–/– mES cell lines were established. Each line had a normal male karyotype (not shown) and displayed the markers of undifferentiated mES cells: high levels of alkaline phosphatase activity (fig. 1 A), expression of SSEA-1 (fig. 1 B), and high levels of Oct-4 protein (fig. 1 C). There was no apparent variability in these characteristics between the cell lines. The presence or absence of p27 protein was confirmed by Western blotting (fig. 1 D). Experiments described here used two p27–/– cell lines (numbers 16 and 22), p27+/+ cell line number 10, and p27+/+ cell line D3 (described previously [17]). To characterize their growth parameters, the cell lines were seeded at low density onto MEF feeder layers and the increase in total protein was monitored daily for 3 days. Along with the lack of any difference in their morphology, no difference between the p27+/+ and p27–/– cell lines was observed with respect to the rate of increase in the protein content accompanying their proliferation (fig. 1 E). Therefore the absence of p27 does not influence a basal proliferation rate of mES cells.

p27-deficient mES cells respond aberrantly to the induction of differentiation

To induce differentiation, mES cells were grown in the absence of LIF from day 0 (D0), and then exposed to RA for 48 h beginning on day 1 (D1) (see fig. 2 A for the schematic). As expected, the amount of p27 was very low in undifferentiated normal mES cells but gradually increased following induction of differentiation (fig. 2 B). To assess the functional significance of this p27 accumulation, differentiation-associated changes were monitored in both normal and p27-deficient mES cells. First, while normal mES cells flattened (by D2) and produced a confluent monolayer (by D4), no such progression was observed in p27–/– mES cells (fig. 2 C). Instead, p27–/– cells became loosely attached to the dish (by D2) and eventually underwent massive cell loss, resulting in only individual cells and/or very small colonies (by D4) at the end of the incubation period. Flow cytometric analysis of detached cells showed that this population consisted predominantly of apoptosing cells and some cellular debris (not shown). Therefore, such floating cells were not subjected to further analyses except for the assays addressing
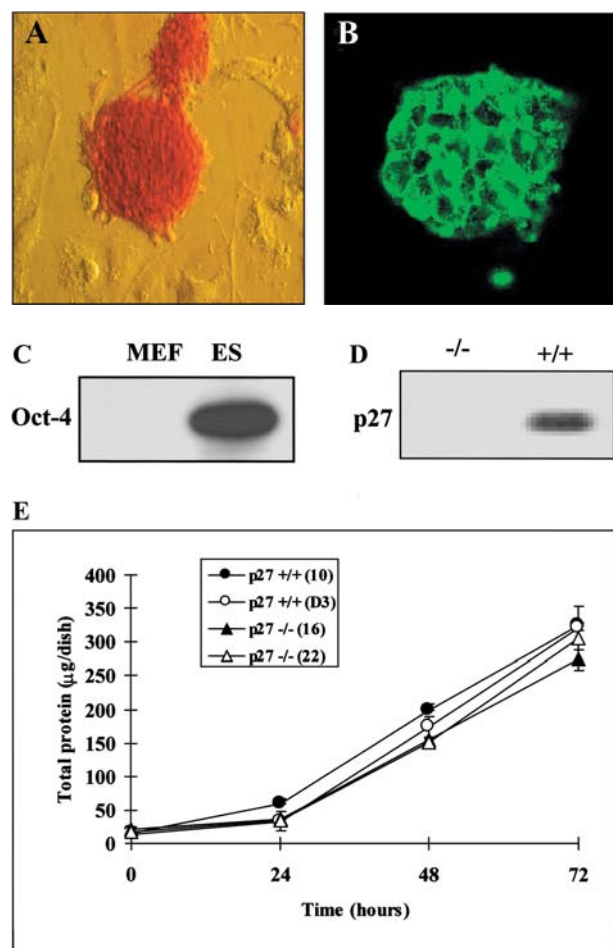
Figure 1. Characterization of established mES cell lines. The newly derived mES cell lines were examined for various markers of undifferentiated mES cells. The activity of alkaline phosphatase (red) (note surrounding feeder cells with lack of activity) (*A*), the expression of SSEA-1 cell surface antigen (green) on mES cells (*B*) as visualized by fluorescence microscopy. (*C*) The expression of Oct-4 protein in MEFs and mES cells as determined by Western blot. Cell line no. 22 deficient for p27 is shown in *A–C*. (*D*) The expression of p27 protein in differentiating p27-deficient mES cells and normal controls as determined by Western blot. (*E*) The total amount of protein from two p27+/+ (no. 10 and D3) and two p27–/– (nos 16 and 22) mES cell lines grown on an MEF feeder layer for 3 days was measured. The averages and standard deviations from three independent replicates are shown.

Figure 2. Effects of the absence of p27 on the differentiation of mES cells. (*A*) A schematic diagram of the differentiation protocol used. At day 0 (D0), LIF was withdrawn from the mES cells. The cells were treated with RA from day 1 (D1) through day 3 (D3). Cells were monitored daily through day 4 (D4). (*B*) The level of p27 protein expressed in normal mES cells during differentiation as determined by Western blot. (*C*) The morphology of normal and p27-deficient cells was monitored by microscopy during differentiation. (*D*) The total amount of protein from two p27+/+ (no. 10 and D3) and two p27–/– (nos 16 and 22) mES cell lines during RA-induced differentiation was analyzed. The mean and standard deviations from three independent replicates are shown.

their apoptotic status (lamin B and PARP cleavage, genomic DNA fragmentation, TUNEL analysis and analysis of mitochondrial membrane potential).

This difference in viability between normal and p27-deficient mES cells was also demonstrated by their growth properties (fig. 2D). Although some cell death was observed in non-mutant cells at days 3 and 4 of differentiation, the cell death observed in p27–/– mES cells was significantly greater, with an almost complete loss of viable cells (between 80 and 95%) at day 4. This precluded analyses of p27–/– cells at day 4 of differentiation.

p27-deficient cells are able to slow cell cycle progression

The results described above suggest that some processes normally associated with the commencement of RA-induced differentiation do not proceed normally in the absence of p27. Because the inhibitory activity of p27 toward cyclin-CDK complexes is well established, we first examined the ability of p27-deficient mES cells to slow their cell division cycle. Surprisingly, differentiation-induced alterations in the percentages of cells in the G1 and S phases of the cell cycle were similar in normal and p27-deficient mES cells (fig. 3A). This result was confirmed by metabolic labeling of newly synthesized DNA with BrdU followed by
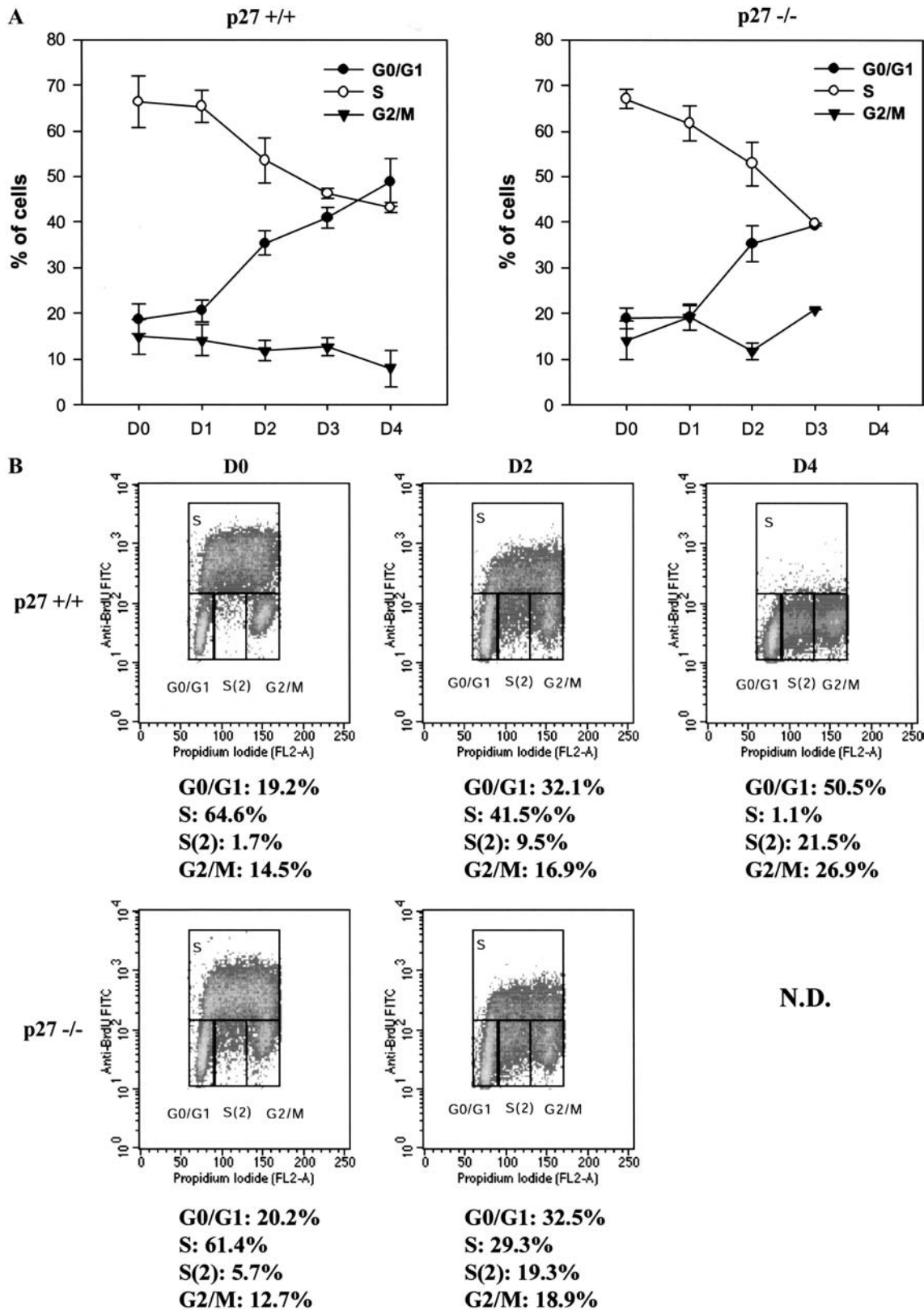
Figure 3. Cell cycle progression of normal and p27-deficient cells. (*A*) The percentage of normal and p27-deficient mES cells in individual cell cycle phases (G0/G1, filled circle; S, open circle; G2, triangle) as determined by flow cytometry. The averages and standard deviations from at least three independent replicates are shown. (*B*) Normal and p27-deficient mES cells at various stages of differentiation were metabolically labeled with BrdU. The cells were stained with PI and FITC-conjugated anti-BrdU antibody and then scored by flow cytometry. The typical plots and the percentage of cells in individual areas are presented.

flow cytometric analysis (fig. 3B). In both normal and p27-deficient mES cells, the percentage of BrdU-labeled cells decreased during differentiation. Although we were unable to quantify DNA synthesis in p27–/– cells at day 4, the decrease that occurs between day 0 and day 2 (from 61.4 to 29.3% BrdU-positive cells) demonstrates that DNA synthesis is down-regulated in p27-deficient mES cells. Therefore, p27 activity is dispensable for inhibition of proliferation in differentiating mES cells.

The absence of p27 affects levels of cyclins D2 and D3
As demonstrated above, the absence of p27 had no significant effect on the proliferation of mES cells. However, the absence of p27 can affect the organization of cell cycle machinery in differentiating mES cells. To address this issue, we analyzed the levels and kinase activities of cyclins and CDKs, their physical associations, and the behavior of p27-related CKI p21. As shown in figure 4, the kinase activities associated with CDK2, cyclin E, and cy-
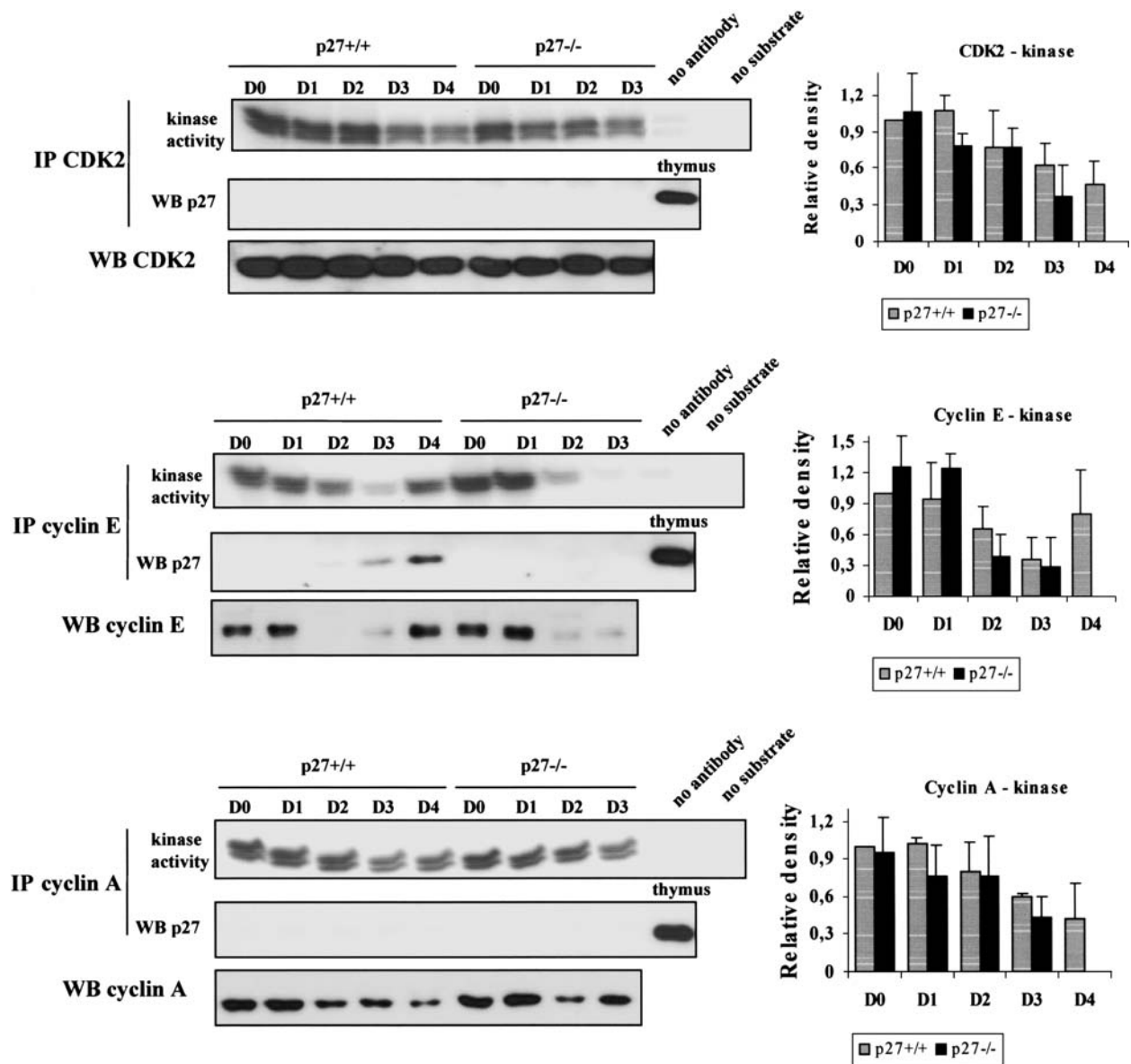
Figure 4. Effects of the absence of p27 on cyclin A/E-CDK2 complexes in differentiating mES cells. Cell lysates from differentiating normal and p27-deficient mES cells were used to immunoprecipitate CDK2, cyclin E, and cyclin A. The kinase activity toward histone H1 was determined by autoradiography and quantified by densitometry. A p27+/+ sample from day 0 (D0) without antibody or histone H1 served as negative controls. The amount of p27 in immunoprecipitates was determined by Western blotting. A sample of thymus proteins served as a positive control in immunoprecipitation studies. The total amount of CDK2, cyclin E, and cyclin A in cells as determined by Western blotting is also presented. The average density of p27+/+ samples from day 0 was defined as 1.0, and from this value all other values were calculated. Data represent the means with standard deviations indicated by error bars. Data are representative of at least three independent replicates.

clin A were similarly decreased in both p27+/+ and p27–/– mES cells following the induction of differentiation. While the levels of cyclin E protein dropped precipitously following the addition of RA (D2 and D3), its levels were restored after RA removal (D4). In contrast, cyclin A protein levels decreased continually, and the levels of CDK2 protein remained essentially unchanged throughout differentiation.

Immunoprecipitation analysis demonstrated detectable amounts of p27 associated with cyclin E only at later stages of differentiation (D3 and D4) (fig. 4). Given that down-regulation of cyclin E-associated kinase activity does not require p27 protein (fig. 4), the levels of cyclins A and E, rather than the inhibitory activity of p27, are likely to be responsible for down-regulation of CDK2 kinase activity in differentiating mES cells.

The patterns of expression of individual D-type cyclin family members differ during differentiation of mES cells (fig. 5A). In undifferentiated, normal mES cells, D1 and D3 but not D2 cyclins were detectable. However, as early as day 2 of differentiation, cyclin D2 protein reached detectable levels. In contrast, differentiation in-

duced a slight decrease in the level of cyclin D1, while no change occurred in the level of cyclin D3. Although p27-deficient mES cells followed a similar pattern of D-type cyclin expression dynamics, the absolute levels of expression were different from those observed in normal mES cells. Specifically, the amounts of cyclins D2 and D3 were much lower in mutant mES cells compared to their normal counterparts. A prototypical partner of D-type cyclins, CDK4, was not subject to any differentiation-associated changes in expression in either normal or mutant mES cells. However, the absence of p27 resulted in abnormalities in activity of CDK4. Compared to normal mES cells, the activity of CDK4 in p27–/– mES cells was generally lower and lacked its transient (although statistically non-significant) surge invariably observed in normal ES cells at days 2 and 3 of differentiation (fig. 5B). Correspondingly, the physical association of cyclin D3 with CDK4, observed in normal mES cells, was absent from their mutant counterparts (fig. 5B). This loss of cyclin D3/CDK4 interaction is likely due to the physical association of cyclin D3 with p27, which occurred in mES cells under normal conditions (fig. 5C). The finding
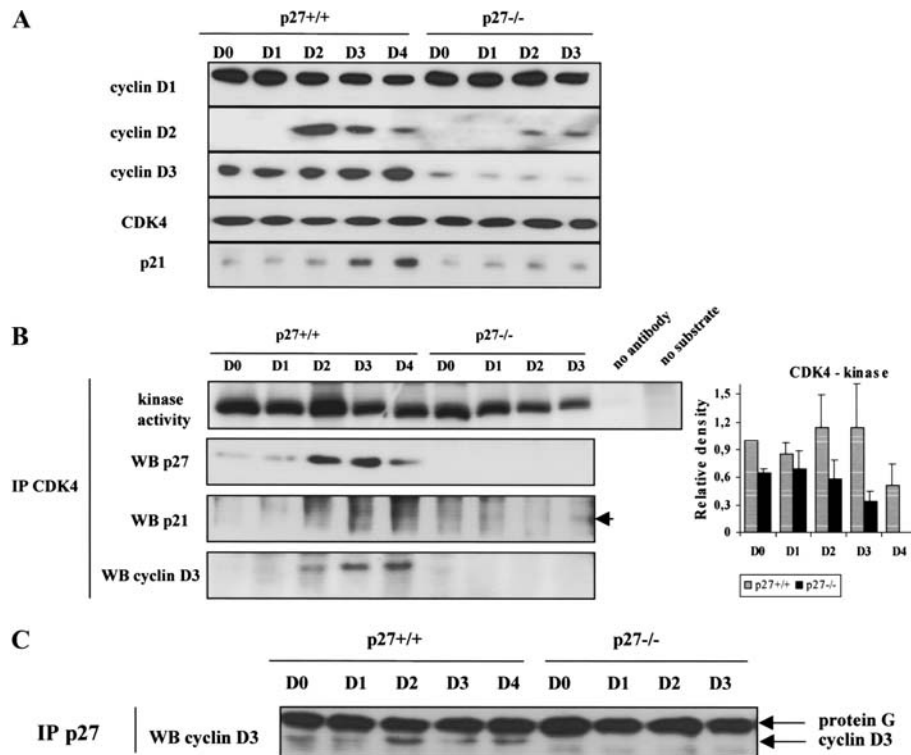
Figure 5. Effects of the absence of p27 on cyclin D-CDK4 complexes in differentiating mES cells. (*A*) Levels of cyclin D1, cyclin D2, cyclin D3, CDK4, and p21 in differentiating normal and p27-deficient mES cells as determined by Western blotting. (*B*) CDK4 was specifically immunoprecipitated from extracts of differentiating normal and p27-deficient mES cells. pRb-specific kinase activity was determined by autoradiography and quantified by densitometry. p27+/+ sample from day 0 (D0) without antibody or GST-pRb served as negative controls. The average density of p27+/+ samples from day 0 was defined as 1.0, and from this value all other values were calculated. Data represent the means with standard deviations indicated by error bars. The amounts of p27, p21, and cyclin D3 in immunoprecipitates were analyzed by Western blots. (*C*) The amount of p27-associated cyclin D was determined by the specific immunoprecipitation of p27 followed by Western blot for cyclin D3. Data are representative of three independent replicates.

that cyclin D3/CDK4 complexes do not form properly in the absence of p27, together with the demonstration that p21 is present in appreciable amounts in p27–/– mES cells (fig. 5 A), suggests that p21 cannot fully compensate for loss of p27 function. These data demonstrate that the absence of p27 indeed causes aberrations in the organization of the cell cycle regulating machinery in mES cells. Specifically, when p27 is unavailable, the activity of CDK4 is lowered, most likely due to the reduced levels of cyclins D2 and D3 altering the amount and/or structure of cyclin-CDK complexes.

p27-deficient mES cells do achieve a differentiated phenotype

As shown above, p27 is not required for mES cells to regulate their proliferation (fig. 3). Here we asked whether or not mES cells are also able to develop a differentiated phenotype in the absence of p27. The morphology of surviving p27-deficient cells (day 4) closely resembled that of normal mES cells as determined by phase contrast microscopy (fig. 6 A) and following E-cadherin staining (fig. 6 B). Additionally, p27-deficient cells expressed cytokeratin Endo A (TROMA-I antibody), a differentiation marker of mouse trophoblast and primitive endoderm [20] typical for derivatives of non-mutant mES cells (fig. 6 C). When cytokeratin Endo-A protein levels were quantified by Western blotting, there was no difference between normal and p27-deficient cells (fig. 6 D). Furthermore, differentiation-associated down-regulation of Oct-4 had the same dynamics in normal and p27-deficient mES cells (fig. 6 D). Taken together, the absence of p27 does not prevent mES cells from developing a fully differentiated phenotype.

p27-deficient mES cells are susceptible to differentiation-associated apoptosis

Cellular differentiation is a complex process requiring considerable restructuring of the intracellular space. The integrity of this process is controlled by the elimination of defective cells via apoptosis, while cells that differentiate properly are protected. To examine the role of p27 in the regulation of apoptosis, we first compared the level of apoptosis in normal and p27–/– cells using the cleavage of nuclear lamin B and the fragmentation of genomic DNA as apoptotic markers. In normal cells, some cleavage of lamin B was transiently detected only at day 3 (fig. 7 A). In contrast, by day 2, cleaved lamin B could be detected in p27-deficient cells, and by day 3, most lamin B was cleaved (fig. 7 A). Similarly, a DNA ladder, reflecting the fragmentation of genomic DNA, was detected only in p27-deficient cells at D2 and D3 (fig. 7 B). This observable increase in apoptosis in p27-deficient mES cells was further analyzed statistically by TUNEL assay applied on populations of attached and attached+floating mES cells. At D3 of differentiation, the proportion of in-
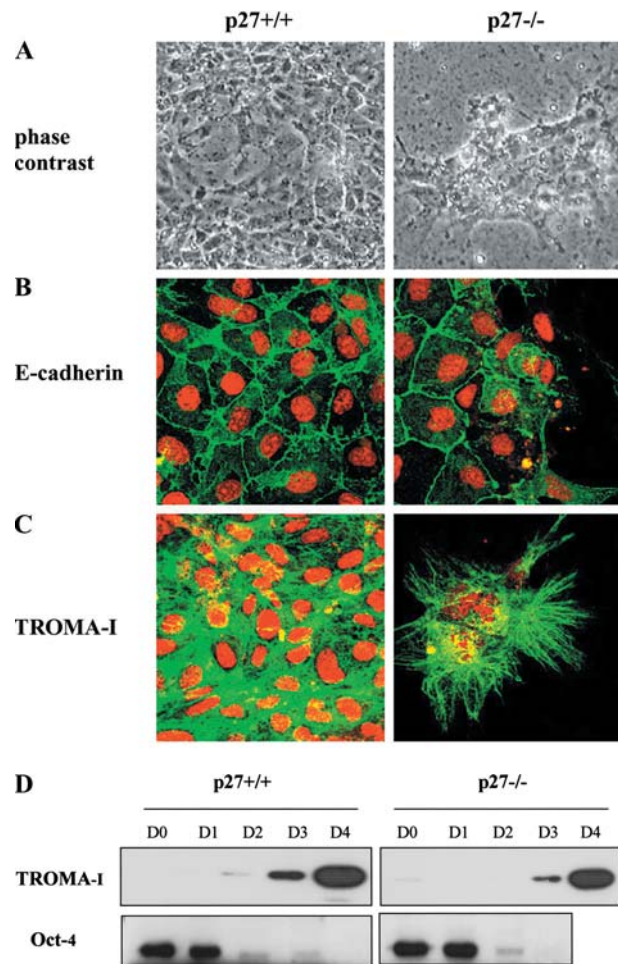
Figure 6. Effects of the absence of p27 on the expression of differentiation markers in mES cells. Mouse ES cells grown on glass cover slips were treated according to the protocol outlined in figure 2A and analyzed at day 4 (D4) (*A*). Cell morphology was analyzed by phase contrast microscopy. The expression of E-cadherin (*B*) and cytokeratin Endo-A (TROMA-I) (*C*) was visualized by indirect immunofluorescence. The amount of cytokeratin Endo-A (TROMA-I) and Oct-4 in differentiating p27+/+ and p27–/– mES cells was analyzed by Western blotting (*D*).

tact (PI-positive) TUNEL-positive cells was almost four times higher in p27-deficient cells than in controls (fig. 8). Together, the results of all three assays clearly demonstrate that the lack of p27 leads to increased apoptosis of mES cells induced to differentiate by RA.

Initiation of differentiation is sufficient for the increased apoptosis to occur in p27-deficient cells

RA is known to induce differentiation at very low concentrations (down to 1×10^{-9} M) but can be toxic to some cell types at higher levels [21]. We tested whether the above-described effect of p27 deficiency on apoptosis could be ascribed to RA toxicity rather than RA-mediated induction of differentiation. Cells were treated with RA at concentrations ranging from 1×10^{-9} to 2×10^{-6} M. Although there was a detectable difference in cellular mor-
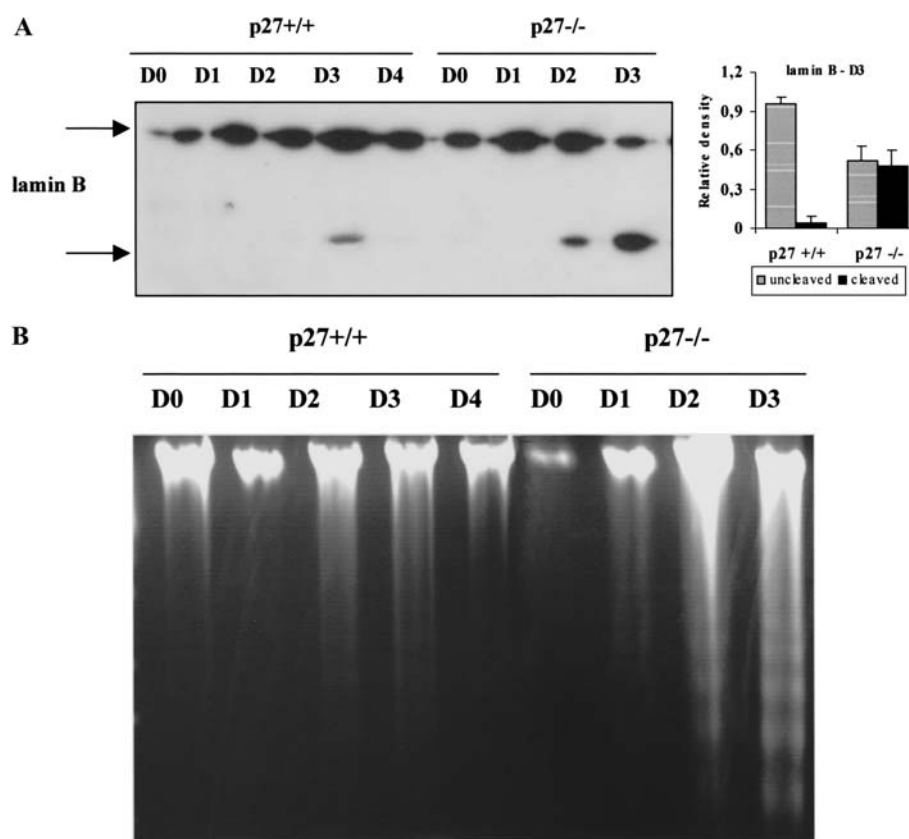
Figure 7. Effects of the absence of p27 on the level of apoptosis in differentiating mES cells. (*A*) Mouse ES cells were treated according to the protocol outlined in figure 2 A. Both floating and attached cells were lysed, and the cleavage of lamin B was determined by Western blotting. Cleavage products at day 3 (D3) were quantified by densitometry. The cumulative density of both bands representing cleaved and uncleaved lamin B in the p27+/+ sample was defined as 1.0, and from this value all other values were calculated. Data represent the means with standard deviations indicated by error bars. (*B*) Genomic DNA from both floating and attached cells was isolated and analyzed on 1.5 % agarose gels. Data are representative of three independent replicates.

phology (fig. 9 A) and cleavage of lamin B (fig. 9 B) between normal and p27-deficient mES cells at all concentrations of RA used, there was no detectable difference in the overall degree of apoptosis in either cell line in response to increasing RA concentrations (fig. 9 A, B). As shown in figure 9 C, more apoptosis was detected in differentiated p27-deficient cells even in the absence of RA. These data suggest that the observed increase in apoptosis in p27-deficient cells is a result of the onset of differentiation rather than being due to the toxicity of RA.

Because p27-deficient cells grow more slowly than normal cells during differentiation (see fig. 2 C), a phenomenon which could lead to reduced cell-cell contacts and the production of intrinsic signals, we next determined if the above-described differences in apoptosis could be an indirect effect of the different growth properties of normal and p27-deficient cells. Cells were seeded at densities between 2×10^4 and 1.5×10^5/cm^2 and treated as previously described (see fig. 2 A). While the extent of cleavage of lamin B differed between p27+/+ and p27–/–mES cells, it was not influenced by cell density within each re-

spective cell line (fig. 9 D). Therefore, the induction of differentiation per se rather then sensitivity to RA or overall cell density is responsible for the observed increased apoptosis in p27-deficient cells. Thus, we infer that the role of up-regulated p27 during differentiation of mES cells involves protection of mES cells from differentiation-associated apoptosis.

Caspase inhibitors fail to prevent apoptosis in mES cells

At least under certain conditions, caspase-dependent pathways are involved in driving apoptosis in mES cells [22, 23]. To address whether or not the activity of caspases is also essential for the observed increase in apoptosis in differentiating p27-deficient mES cells, both normal and p27-deficient cells were treated with a general caspase inhibitor (zVAD-fmk), a caspase 3-specific inhibitor (z-DEVD-fmk), and a caspase 6-specific inhibitor (zVEID-fmk). None of these inhibitors caused significant changes in morphology and/or growth parameters of mES cells when analyzed at day 3 of differentiation (not

Attached cells
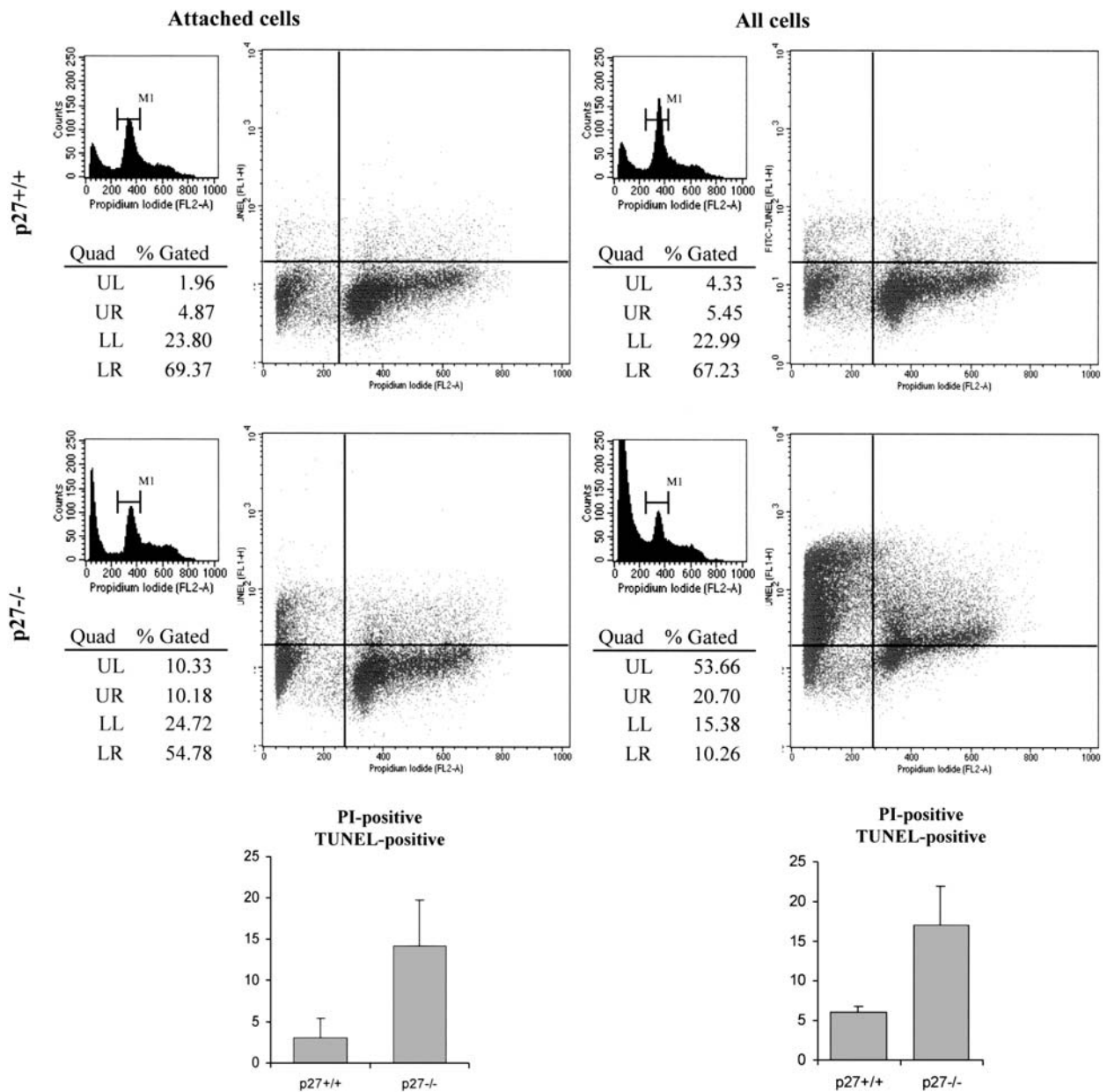
All cells

Figure 8. TUNEL analysis of differentiating normal and p27-deficient mES cells. Mouse ES cells were treated according to the protocol outlined in figure 2 A. At day 3 (D3), both attached and attached+floating (all) cells were subjected to TUNEL assay followed by flow cytometric analysis. The typical plots and the percentages of cells in individual areas are presented. PI- and TUNEL-positive cells (upper right quadrant) were considered to be intact apoptotic cells and their quantification is presented in the graphs below as the means plus standard deviation.

shown). Correspondingly, such treatments did not affect the cleavage of lamin B and PARP, both of which are substrates for caspases (fig. 10).

p27–/– mES cells do not show major abnormalities in the metabolism of specific anti- and pro-apoptotic proteins

The progression of apoptosis in cells is modulated by the activities of several anti- and pro-apoptotic proteins [for a review see ref. 24]. To identify those molecular pathways

responsible for the enhanced apoptosis observed here, the levels of some of these proteins were determined in normal and p27-deficient mES cells. From the total of eight proteins analyzed, only Bcl-2, Bcl-X$_L$, and Bag-1 (all anti-apoptotic), and Bak and Bad (both pro-apoptotic) were detectable in mES cells. Another three proteins, pro-apoptotic Bid (sc-6538) and Bax (B31420), and anti-apoptotic protein Mcl-1 (M8434) were undetectable under any assay condition (not shown). Most important, these proteins showed no p27 genotype-related anomalies
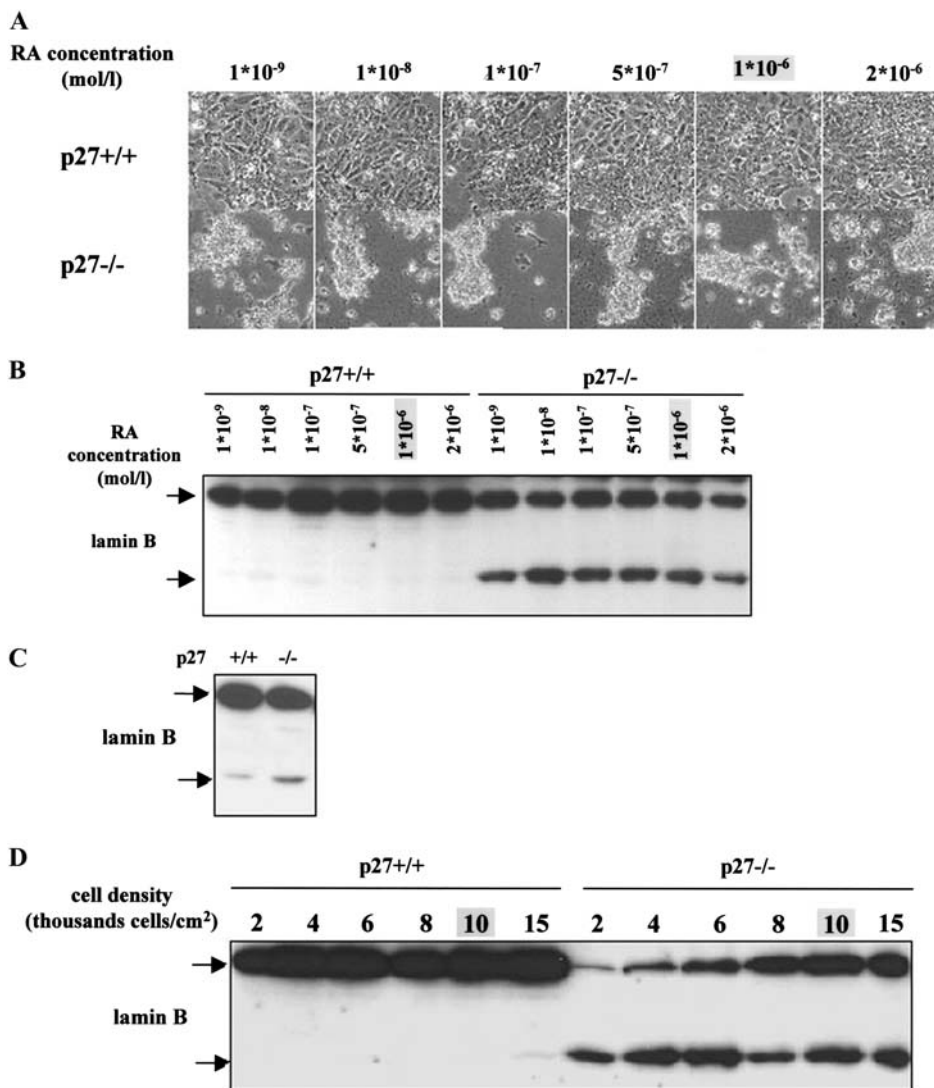
Figure 9. The effect of RA concentration and cell density on apoptosis in differentiating normal and p27-deficient mES cells. Mouse ES cells were treated according to the protocol outlined in figure 2 A with different concentrations of RA and then analyzed by phase contrast microscopy at day 3 (D3) (*A*). Both floating and attached cells were lysed at day 3, and the cleavage of lamin B was determined by Western blotting (*B*). Mouse ES cells were differentiated in the absence of LIF for 3 days. The cleavage of lamin B was determined by Western blotting (*C*). Mouse ES cells were seeded at densities from 2000 to 15,000 cells/cm^2 and treated according to the protocol outlined in figure 2 A. Both floating and attached cells were lysed and the cleavage of lamin B was analyzed by Western blotting (*D*).

in their respective amounts during mES cell differentiation (fig. 11). Although a slight increase in the amounts of Bcl-X$_L$ and Bad in p27–/– cells was observed in some experiments, we were unable to statistically prove such accumulations to be significant.

Overexpressed cyclin D3 guards p27-deficient mES cells against increased apoptosis

Down-regulation of cyclin D3 has previously been shown to be involved in driving apoptosis in various cell types [25–28]. Here, p27-deficient mES cells, which were highly prone to apoptosis, were characterized by dramatically reduced levels of cyclins D2 and D3 (see fig. 5). This raises the question as to whether down-regulation of

D-type cyclin contributes to the pro-apoptotic phenotype of p27–/– mES cells, and plasmid-driven expression of cyclin D3, the most abundant D-type cyclin in mES cells, was used to address this question. Cells were cotransfected with a mixture (1:8) of pEGFP-C1 and pNeo-CycD3 expression vectors [10]. EGFP-positive cells were considered to express also exogenous cyclin D3 from pNeoCycD3. After 2 days of RA-induced differentiation as above, the level of apoptosis in GFP-positive cells was determined by flow cytometry, using the mitochondrial membrane potential ($\Delta\Psi_m$) as a marker. As shown in figure 12, overexpression of cyclin D3 resulted directly in reduced apoptosis in p27–/– mES cells, as well as in their normal counterparts. These data provide a functional link
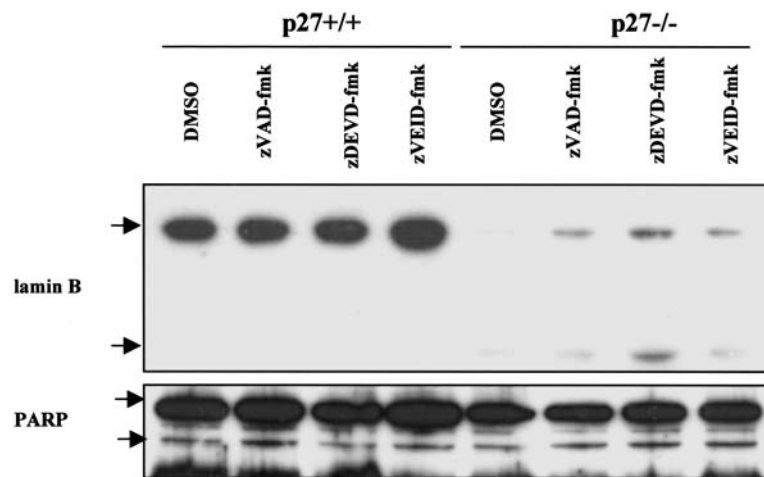
Figure 10. The effect of caspase inhibitors on apoptosis in normal and p27-deficient mES cells. mES cells were treated according to the protocol outlined in figure 2 A. At D1, cells were treated with DMSO (control solvent), a general a caspase inhibitor (zVAD-fmk), caspase 3-specific inhibitor (z-DEVD-fmk), and a caspase 6-specific inhibitor (zVEID-fmk). Both floating and attached cells were lysed at D3 and the cleavage of lamin B and PARP was analyzed by Western blot.
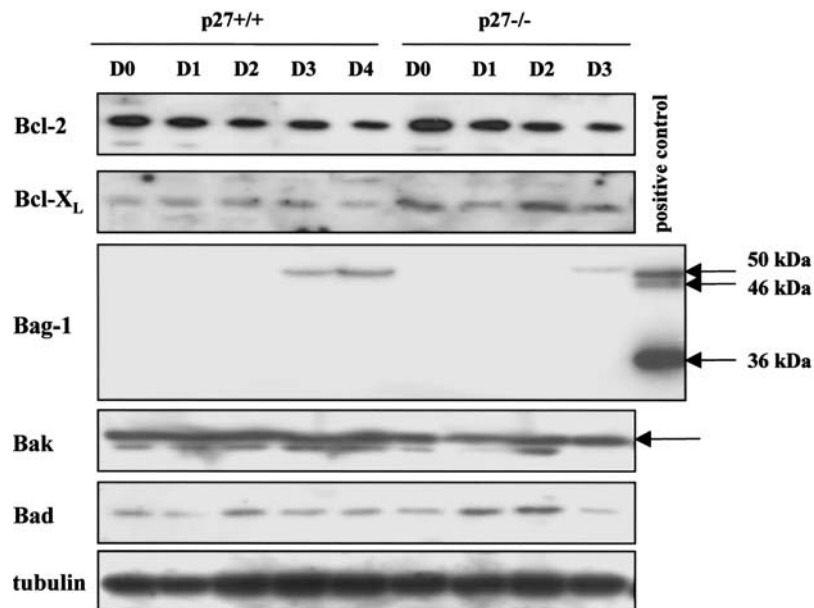
Figure 11. Expression of proteins regulating apoptosis in differentiating normal and p27-deficient mES cells. Extracts were prepared from normal and p27-deficient mES cells at various stages of differentiation and the levels of Bcl-2, Bcl-X$_L$, Bag-1, Bak, and Bad proteins were analyzed by Western blotting. Alpha-tubulin was used as a loading control. HL-60 cells were used as a positive control for Bag-1.

between the levels of D-type cyclins and the promotion of apoptosis in mES cells.

Discussion

The differentiation of cells of early embryonic origin is a complex process by which highly proliferating, self-renewing cells switch their developmental program to differentiation. This critical event is usually accompanied by reduced proliferation. One common feature of differenti-

ated early embryonic cells is elevated Cip/Kip inhibitor p27 protein [5–13]. To assess the role of p27 in embryonic differentiation, we used adherent cultures of both normal and p27-deficient mES cells in which differentiation was induced by withdrawal of LIF combined with the RA treatment [14]. Using this system, we analyzed the effects of p27 on several well-established characteristics of mES cell differentiation. The extent to which p27 is required for differentiation signal-associated inhibition of proliferation and differentiation sensu stricto was examined. Because the formation of tissues and organs within
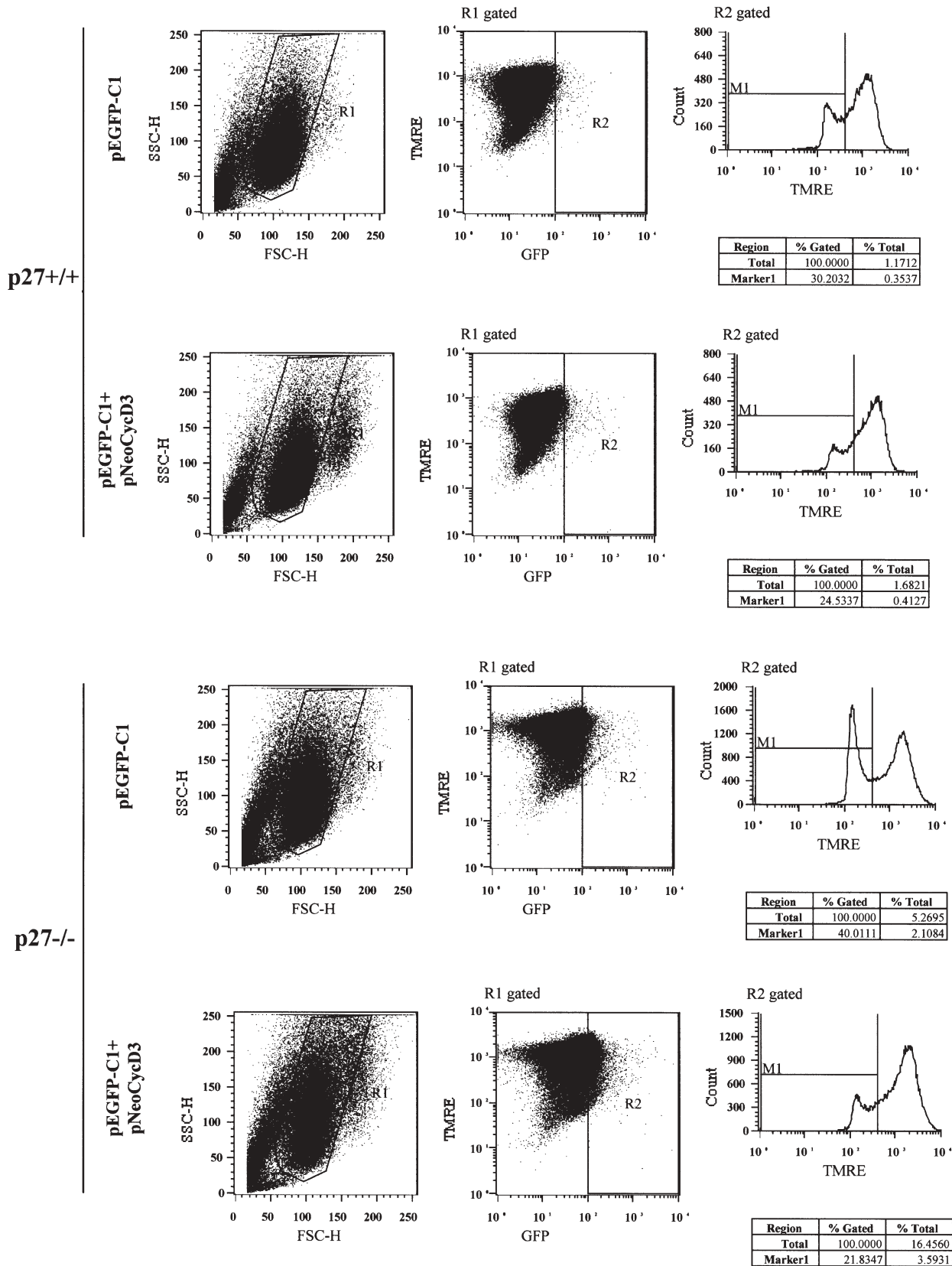
Figure 12. The effect of overexpressed cyclin D3 on apoptosis in differentiating normal and p27-deficient mES cells. Normal and p27-deficient mES cells were electroporated with pEGFP-C1 with or without pNeoCycD3 expression vector. Transfected cells were differentiated according to the protocol outlined in figure 2A. At day 2 (D2) of differentiation, the apoptosis in EGFP-positive cells was quantified using flow cytometric analysis of mitochondrial membrane potential (TMRE). Marker 1-gated cells were considered to be apoptotic.

the early mammalian embryo is tightly associated with programmed cell death, we also analyzed the level of apoptosis in normal and p27-deficient mES cells stimulated to differentiate.

We have demonstrated that the absence of p27 does not affect the ability of mouse ES cells to properly slow cell cycle progression. When compared to normal mES cells, cell cycle distribution, DNA synthesis, and the activity of the key CDKs that regulate G1/S entry are unaffected in differentiating p27-deficient mES cells. Cip/Kip family members inhibit active cyclin-CDK [29] complexes resulting in a suspension of cellular proliferation. Although p27 becomes increasingly associated with cyclin E and CDK4 during differentiation, the absence of p27 does not significantly alter their associated kinase activities. Therefore, the activities of CDK2 and CDK4 seem to be regulated predominantly at the level of cyclin availability. Savatier and colleagues [5] have shown that overexpression of p27 in both proliferating and differentiated mES cells leads to cell cycle arrest. Correspondingly, artificial down-regulation of p27 in human NTERA-2 EC cells induced to differentiate by hexamethylene-bisacetamide (HMBA) [13] or RA [6] causes defects in cell cycle breaking. However, here, p27 was not required for the inhibition of proliferation of mES cells associated with differentiation induced by LIF withdrawal combined with RA treatment. The biological role of p27 in differentiating cells of early embryonic origin thus seems to differ depending on the differentiation pathway. The differences between individual cell lines can represent another source of variability. Savatier and colleagues [5] showed that the levels of D-type cyclins and CDK4-associatied kinase activity are very low in CGR8 mES cells. In contrast, in our newly established mES cells and also in the D3 line of mES cells (not shown), CDK4-associated kinase activity as well as the levels of cyclin D1 and D3 are quite high.

The p27-deficient mES cells progressively die after LIF withdrawal combined with RA treatment. However, surviving p27-deficient cells have a comparable phenotype to differentiated normal cells. Our results thus differ from the conclusions of others that elevated p27 in EC cells contributes to the regulation of differentiation [6, 11, 13]. However, the process of differentiation may differ between individual EC and mES cell lines, and the role of p27 may differ depending on the differentiation signal and/or manner. Currently, studies where p27-deficient mES cells are induced to differentiate using other protocols are in progress to clarify the general role of p27 in early development.

Analyses of nuclear lamin B, fragmentation of genomic DNA (DNA ladder and TUNEL assay), and mitochondrial membrane potential demonstrate that differentiating p27-deficient mES cells are dying via apoptosis. The extent of apoptosis did not increase with increasing concentrations of RA or cell density, suggesting that the onset of differentiation itself is a sufficient signal for cells to enter the apoptotic pathway. Importantly, while mES cells are able to fully compensate for the lack of p27 with respect to cell cycle regulation, they cannot compensate for the function of p27 required to protect against cell death. These data suggest that p27 is the crucial component of the apoptosis protection mechanism in differentiating mES cells.

The up-regulation of p27 in cancer cells is typically connected with its ability to induce cell cycle arrest and promote apoptosis [for reviews see ref. 30, 31]. In contrast, p27 has been found to be anti-apoptotic in other cellular models [32−41]. There were two previous studies on the role of p27 in mouse teratocarcinoma-derived EC cells. Using a p27 antisense oligonucleotide strategy, Glozak and Rogers [8] demonstrated that RA- and bone morphogenetic protein 4 (BMP-4)-induced apoptosis in P19 EC cells required p27. In contrast, Baldassarre and colleagues [13] showed that down-regulation of p27 by specific antisense oligonucleotides leads to massive programmed cell death of human NT2/D1 EC cells induced to differentiate by HMBA. Important to note is that three-dimensional cell culture was used by Glozak and Rogers while monolayer culture was employed in this study and in the study of Baldassarre. Recently, we observed abnormal development in embryoid bodies produced from p27–/– ES cells, with one cell lineage being eliminated due to increased apoptosis, while the other was expanded, possibly thanks to its lower sensitivity to the absence of p27 [unpublished data]. Therefore, cell type-specific functioning of p27 may well explain the occurrence of both pro- and anti-apoptotic effects of p27 in differentiating pluripotent cells.

Two specific molecular events that were previously shown to result from the absence of p27, hyperactivation of CDK2 and CDK4 kinases [42] and down-regulation of D-type cyclins [43−45], were also found to be associated with the induction of programmed cell death in many cell types [25−28, 35, 36, 46−51]. In this study, neither CDK2- nor CDK4-associated kinase activities were altered in the absence of p27, and therefore could not contribute to elevated apoptosis in p27-deficient mES cells. In contrast, the levels of both cyclin D2 and cyclin D3 were lowered dramatically in p27-deficient mES cells compared to their wild-type counterparts. Moreover, over-expression of cyclin D3 significantly reduced differentiation-associated apoptosis both in wild-type and p27-deficient mES cells. A similar protective effect was observed following overexpression of cyclin D2 and D3 in WEHI 231 and Jurkat cells, respectively [25, 26]. Taken together, although our study does not provide a specific molecular mechanism or pathway by which p27 protects mES cells from differentiation-associated apoptosis, the data suggest that the role of p27 in maintaining appropriate levels of cyclin D3 (and cyclin D2) is at least in part responsible for its anti-apoptotic activity.

Joza and colleagues [52] recently demonstrated that the activity of apoptosis-inducing factor (AIF) is required for programmed cell death in embryoid bodies produced from mES cells. Crucially, this AIF-dependent apoptotic pathway, which is essential for cell death occurring normally during early development in mammals, does not involve the action of caspases. When in this study the activity of caspases was chemically inhibited in apoptosing p27-deficient mES cells, none of the parameters of apoptosis was significantly affected. Correspondingly, the absence of p27 caused no disturbances in the metabolism of the selected pro- and anti-apoptotic proteins functionally linked to the caspase-dependent pathway. We infer that caspase-independent apoptotic pathway(s) are responsible for the massive cell death of differentiating p27-deficient mES cells, with the AIF-dependent pathway being the most likely candidate.

Our study on p27-deficient mES cells stimulated to differentiate expands the current understanding of cell cycle regulation in cells of embryonic origin. Our data indicate that p27 plays a greater role in differentiating mES cell survival than in regulating cell cycle progression. We propose that the processes that control cell cycle regulation and apoptosis in mES cells are linked via p27 and cyclin D3.

1 Evans M. J. and Kaufman M. H. (1981) Establishment in culture of pluripotential cells from mouse embryo. Nature **292:** 154–156

2 Martin G. R. (1981) Isolation of a pluripotent cell line from early mouse embryos cultured in medium conditioned by teratocarcinoma stem cells. Proc. Natl. Acad. Sci. USA **28:** 7634–7638

3 Smith A. (2001) Embryonic stem cells. In: Stem Cell Biology, pp. 205–230, Marshak D. R., Gardner R. L. and Gottlieb D. (eds), New York, Cold Spring Harbor Laboratory Press

4 Kelly D. L. and Rizzino A. (2000) DNA microarray analyses of genes regulated during the differentiation of embryonic stem cells. Mol. Reprod. Dev. **56:** 113–123

5 Savatier P., Lapillonne H., Grunsven L. A. van, Rudkin B. B. and Samarut J. (1995) Withdrawal of differentiation inhibitory activity/leukemia inhibitory factor up-regulates D-type cyclins and cyclin-dependent kinase inhibitors in mouse embryonic stem cells. Oncogene **12:** 309–322

6 Baldassarre G., Boccia A., Bruni P., Sandomenico C., Barone M. V., Pepe S. et al. (2000) Retinoic acid induces neuronal differentiation of embryonal carcinoma cells by reducing proteasome-dependent proteolysis of the cyclin-dependent inhibitor p27. Cell Growth Differ. **11:** 517–526

7 Gill M. R., Slack R., Kiess M. and Hamel P. A. (1998) Regulation of expression and activity of distinct pRB, E2F, D-type cyclin, and CKI family members during terminal differentiation of P19 cells. Exp. Cell Res. **244:** 157–170

8 Glozak M. A. and Rogers M. B. (2001) Retinoic acid- and bone morphogenetic protein 4-induced apoptosis in P19 embryonal carcinoma cells requires p27. Exp. Cell Res. **268:** 128–138

9 Li Y., Glozak M. A., Smith S. M. and Rogers M. B. (1999) The expression and activity of D-type cyclins in F9 embryonal carcinoma cells: modulation of growth by RXR-selective retinoids. Exp. Cell. Res. **253:** 372–384

10 Preclikova H., Bryja V., Pachernik J., Krejci P., Dvorak P. and Hampl A. (2002) Early cycling-independent changes to p27, cyclin D2, and cyclin D3 in differentiating mouse embryonal carcinoma cells. Cell Growth Differ. **13:** 421–430

11 Sasaki K., Tamura S., Tachibana H., Sugita M., Gao Y., Furuyama J. I. et al. (2000) Expression and role of p27[kip1] in neuronal differentiation of embryonal carcinoma cells. Mol. Brain Res. **77:** 209–221

12 Watanabe Y., Watanabe T., Kitagawa M., Taya Y., Nakayama K. and Motoyama N. (1999) pRb phosphorylation is regulated differentially by cyclin-dependent kinase (Cdk) 2 and Cdk4 in retinoic acid-induced neuronal differentiation of P19 cells. Brain Res. **842:** 342-350

13 Baldassarre G., Barone M. V., Belleti B., Sandomenico C., Bruni P., Spiezia S. et al. (1999) Key role of the cyclin-dependent kinase inhibitor p27[kip1] for embryonal carcinoma cell survival and differentiation. Oncogene **18:** 6241–6251

14 Mummery C. L., Feyen A., Freund E. and Shen S. (1990) Characterisics of embryonic stem cell differentiation: a comparison with two embryonal carcinoma cell lines. Cell Differ. Dev. **30:** 195–206

15 Fero M. L., Rivkin M., Tasch M., Porter P., Carow C. E., Firpo E. et al. (1996) A syndrome of multiorgan hyperplasia with features of gigantism, tumorigenesis, and female sterility in p27[Kip1]-deficient mice. Cell **85:** 733–744

16 Hogan B., Beddington R., Costantini F. and Lacy E. (1994). Manipulating the Mouse Embryo: a Laboratory Manual, New York, Cold Spring Harbor Laboratory Press

17 Doetschman T. C., Eistetter H., Katz M., Schmidt W. and Kemler R. (1985) The in vitro development of blastocyst-derived embryonic stem cell lines: formation of visceral yolk sac, blood islands and myocardium. J. Embryol. Exp. Morphol. **87:** 27–45

18 Vindelov L. L. (1977) Flow microfluorometric analysis of nuclear DNA in cells from solid tumors and cell suspensions: a new method for rapid isolation and staining of nuclei. Virchows Arch. B. Cell. Pathol. **24:** 227–242

19 Bryja V., Pachernik J., Kubala L., Hampl A. and Dvorak P. (2003) The reverse tetracycline-controlled transactivator rtTA2[S]-S2 is toxic in mouse embryonic stem cells. Reprod. Nutr. Dev. **43:** 477–486

20 Brulet P., Babinet C., Kemler R. and Jacob F. (1980) Monoclonal antibodies against trophectoderm-specific markers during mouse blastocyst formation. Proc. Natl. Acad. Sci. USA **77:** 4113–4117

21 Rohwedel J., Guan K. and Wobus A. M. (1999) Induction of cellular differentiation by retinoic acid in vitro. Cells Tissues Organs **165:** 190–202

22 Hakem R., Hakem A., Duncan G. S., Henderson J. T., Woo M., Soengas M. S. et al. (1998) Differential requirement for caspase 9 in apoptotic pathways in vivo. Cell **94:** 339–352

23 Woo M., Hakem R., Soengas M. S., Duncan G. S., Shahinian A., Kägi D. et al. (1998) Essential contribution of caspase 3/CPP32 to apoptosis and its associated nuclear changes. Genes Dev. **12:** 806–819

24 Cory S., Huang D. C. and Adams J. M. (2003) The Bcl-2 family: roles in cell survival and oncogenesis. Oncogene **22:** 8590–8607

25 Banerji L., Glassford J., Lea N. C., Thomas N. S. B., Klaus G. G. B. and Lam E. W. F. (2001) BCR signals target p27[Kip1] and

cyclin D2 via the PI3-K signalling pathway to mediate cell cycle arrest and apoptosis of WEHI 231 B cells. Oncogene **20:** 7352–7367

26 Boonen G. J. J. C., Oirschot B. A. van, Diepen A. van, Mackus W. J. M., Verdonck L. F., Rijksen G. et al. (1999) Cyclin D3 regulates proliferation and apoptosis of leukemic T cell lines. J. Biol. Chem. **274:** 34676–34682

27 Tan A., Bitterman P., Sonenberg N., Peterson M. and Polunovsky V. (2000) Inhibition of Myc-dependent apoptosis by eukaryotic translation initiation factor 4E requires cyclin D1. Oncogene **19:** 1437–1447

28 Wang P., Pavletic Z. S. and Joshi S. S. (2002) Increased apoptosis in B-chronic lymphocytic leukemia cells as a result of cyclin D3 down regulation. Leukemia Lymphoma **43:** 1827–1835

29 Sherr C. J. and Roberts J. M. (1995) Inhibitors of mammalian G_1 cyclin-dependent kinases. Genes Dev. **9:** 1149–1163

30 Lloyd R. V., Erickson L. A., Jin L., Kulig E., Qian X., Cheville J. C. et al. (1998) p27kip1: a multifunctional cyclin-dependent kinase inhibitor with prognostic significance in human cancers. Am. J. Pathol. **154:** 313–323

31 Philipp-Staheli J., Payne S. R. and Kemp C. J. (2001) p27Kip1: regulation and function of a haploinsufficient tumor suppressor and its misregulation in cancer. Exp. Cell. Res. **264:** 148–168

32 Coqueret O. (2003) New roles for p21 and p27 cell-cycle inhibitors: a function for each cell compartment? Trends Cell Biol. **13:** 65–70

33 Eymin B., Haugg M., Droin N., Sordet O., Dimanche-Boitrel M. T. and Solary E. (1999) p27Kip1 induces drug resistance by preventing apoptosis upstream of cytochrome c release and procaspase-3 activation in leukemic cells. Oncogene **18:** 1411–1418

34 Eymin B., Sordet O., Droin N., Munsch B., Haugg M., Van de Craen M. et al. (1999) Caspase-induced proteolysis of the cyclin-dependent kinase inhibitor p27Kip1 mediates its anti-apoptotic activity. Oncogene **18:** 4839–4847

35 Gil-Gómez G., Berns A. and Brady H. J. M. (1998) A link between cell cycle and cell death: Bax and Bcl-2 modulate Cdk2 activation during thymocyte apoptosis. EMBO J. **17:** 7209–7218

36 Hiromura K., Pippin J. W., Fero M. L., Roberts J. M. and Shankland S. J. (1999) Modulation of apoptosis by the cyclin-dependent kinase inhibitor p27Kip1. J. Clin. Invest. **103:** 597–604

37 Frost V. and Sinclair A. J. (2000) p27KIP1 is down-regulated by two different mechanisms in human lymphoid cells undergoing apoptosis. Oncogene **19:** 3115–3120

38 Masuda A., Osada H., Yatabe Y., Kozaki K., Tatematsu Y., Takahashi T. et al. (2001) Protective function of p27KIP1 against apoptosis in small cell lung cancer cells in unfavorable microenvironments. Am. J. Pathol. **158:** 87–96

39 Ophascharoensuk V., Fero M. L., Hughes J., Roberts J. M. and Shankland S. J. (1998) The cyclin-dependent kinase inhibitor p27Kip1safeguards against inflammatory injury. Nat. Med. **4:** 575–580

40 Tang P. P., Hsieh S. C. and Wang F. F. (2002) Modulation of caspase activation and p27Kip1 degradation in the p53-induced apoptosis in IW32 erythroleukemia cells. Cell. Signal. **14:** 961–968

41 Zindy F., Cunningham J. J., Sherr C. J., Jogal S., Smeyne S., Smeyne R. J. et al. (1999) Postnatal neuronal proliferation in mice lacking Ink4d and Kip1 inhibitors of cyclin-dependent kinases. Proc. Natl. Acad. Sci. USA **96:** 13462–13467

42 Nakayama K., Ishida N., Shirane M., Inomata A., Inoue T., Shishido N. et al. (1996) Mice lacking p27Kip1 display increased body size, multiple organ hyperplasia, retinal dysplasia and pituitary tumors. Cell **85:** 707–720

43 Cheng M., Olivier P., Diehl J. A., Fero M., Roussel M. F., Roberts J. M. et al. (1999) The p21Cip1 and p27Kip1 'inhibitors' are essential activators of cyclin D-dependent kinases in murine fibroblasts. EMBO J. **18:** 1571–1583

44 Bagui T. K., Jackson R. J., Agrawal D. and Pledger W. J. (2000) Analysis of cyclin D3-cdk4 complexes in fibroblasts expressing and lacking p27kip1 and p21cip1. Mol. Cell. Biol. **20:** 8748–8757

45 Bryja V., Pacherník J., Faldíková L., Krejčí P., Pogue R., Nevřivá I. et al. (in press) The role of p27Kip1 in maintaining the levels of D-type cyclins in vivo. BBA Mol. Cell. Res.

46 Adachi S., Ito H., Tamamori-Adachi M., Ono Y., Nozato T., Abe S. et al. (2001) Cyclin A/cdk2 activation is involved in hypoxia-induced apoptosis in cardiomyocytes. Circ. Res. **88:** 408–414

47 Choi K. S., Eom Y. W., Kang Y., Ha M. J., Rhee H., Yoon J.-W. et al. (1999) Cdc2 and Cdk2 kinase activated by transforming growth factor-b1 trigger apoptosis through the phosphorylation of retinoblastoma protein in FaO hepatoma cells. J. Biol. Chem. **274:** 31775–31783

48 Dou Q. P., An B. and Yu C. (1995) Activation of cyclin E-dependent kinase by DNA-damage signals during apoptosis. Biochem. Biophys. Res. Commun. **214:** 771–780

49 Levkau B., Koyama H., Raines E. W., Clurman B. E., Herren B., Orth K. et al. (1998) Cleavage of p21Cip1/Waf1 and p27Kip1 mediates apoptosis in endothelial cells through activation of Cdk2: role of a caspase cascade. Mol. Cell **1:** 553–563

50 Meikrantz W. and Schlegel R. (1996) Suppression of apoptosis by dominant negative mutants of cyclin-dependent protein kinases. J. Biol. Chem. **271:** 10205–10209

51 Park D. S., Morris E. J., Bremner R., Keramaris E., Padmanabhan J., Rosenbaum M. et al. (2000) Involvement of retinoblastoma family members and E2F/DP complexes in the death of neurons evoked by DNA damage. J. Neurosci. **20:** 3104–3114

52 Joza N., Susin S. A., Daugas E., Stanford W. L., Cho S. K., Li C. Y. J. et al. (2001) Essential role of the mitochondrial apoptosis-inducing factor in programmed cell death. Nature **410:** 549–554